

Top quark spin in 2HDM models

Alberto Prades Ibáñez, University of Valencia, Spain

Supervisors: Cecile Deterre and Roger Naranjo (DESY ATLAS Group)

September 6, 2017

Abstract

The SM is a powerful theory that describes an enormous variety of physics processes. However, it has limitations that points to the necessity of searching more completed theories. In many of them, the top quark plays an important role due to its great mass. In this project, we have worked with a simple extension of the SM Higgs, the Two Higgs-Doublet Model (2HDM). This model proposes five Higgs boson and two of them contribute to the production of $t\bar{t}$ pair. Our aim is, using a new set of polarization of spin correlation observables, to perform comprisons between 2HDM predictions and ATLAS data to exclude or constrain the free parameters of this model.

Contents

1	Introduction	3
2	Theory	4
2.1	The Top Quark	4
2.2	Two-Higgs-Doublet model	4
2.3	Polarization and spin correlation	8
2.4	Chi-squared test with correlations between the bins	11
3	Results and discussion	12
3.1	Compatibility between the SM and the 2HDM	12
3.2	Compatibility between the ATLAS data and the different models	16
4	Conclusions	19
	References	24

1 Introduction

The Standard Model of particle physics (SM) is a quantum field theory that describes the elementary particles and their interactions at a subatomic level. The SM assumes that all matter is formed by elementary particles that are characterized by their quantum numbers. The elementary particles are classified in two types according to the SM: fermions (spin $\frac{1}{2}$, described by the Fermi-Dirac statistics) and bosons (integer spin, described by the Bose-Einstein statistics). Fermions are divided into three families formed by three charged leptons, three neutrinos, and six quarks. For each of these particles, there exists an antiparticle with the same mass and opposite quantum numbers. This gives a total of 24 fermionic particles. The bosons are classified into two groups, those which are associated with fundamental interactions between fermions, and the Higgs boson. There are three fundamental interactions in the SM: the strong force, the weak force and the electromagnetism mediated by the gluon (g), the bosons W^\pm , Z and the photon respectively. The Higgs boson is responsible for the mass of the particles [1, 2, 3].

The SM is a powerful theory that describes an enormous variety of physics processes. However, it has limitations that points to the necessity of searching more completed theories. These new theories might unify weak and strong interactions with gravity (which is not included in the SM). Moreover, the SM does not explain the neutrino masses [4] and there is no candidate for dark matter.

Theories Beyond the Standard Model (BSM) propose new ways to solve these limitations. For example, supersymmetry (SUSY) [5] proposes the existence of a supersymmetric particle for each particle of the SM. This theory solves some problems of the SM like renormalization and it gives a candidate for dark matter. Other theories, like the Great Unification Theories (GUT), try to unify the three interactions described by the SM in a unique interaction at high energies and predict the existence of new bosons such as Z' and W' . It also explains the masses of the neutrinos [6, 7].

A way for testing these theories is studying the properties of particles. For example, a set of observables that characterize the top spin structure were proposed in [9] and measured, for the first time, by the ATLAS collaboration [10] that have not been compared yet with BSM theories.

In this report we compare the behaviour of those observables in the SM with one class of BSM models, the two Higgs-Doublet model (2HDM). We also compare the measured values with the predictions of all those models to try to constrain the free parameters of the 2HDM that we study.

2 Theory

2.1 The Top Quark

The top quark is a fermion of spin $s = 1/2$ and charge $Q = +2/3$ discovered at Fermilab in 1995 [11, 12]. It was predicted by the Standard Model as the companion of isospin of the bottom quark belonging to the third generation of fermions. It is the heaviest elementary particle of the SM. Its mass is about 35 times the mass of the second heaviest quark (the bottom quark). This very large mass comes from the coupling with the Higgs boson (the top quark has the highest coupling with this boson). A more detailed explanation of its properties can be found in the Particle Data Group book [1].

Since the lifetime of the top quark is $\simeq 0.5 \cdot 10^{-24} s$ and the typical hadronization time is $\simeq 3 fm/c \simeq 3.3 \cdot 10^{-24} s$ [13], the top quark decays before hadronization and before any consequent spin-flip can take place. This offers a unique opportunity to study the properties of a bare quark and the properties of its spin.

At hadron colliders, top quarks are mainly produced in $t\bar{t}$ pairs via the strong interaction. The quarks and gluons of the initial state are unpolarised, which means that their spins are not preferentially aligned with any given direction. The top quarks produced via QCD are expected to be almost unpolarized but their spins are expected to be correlated. The spins of the top quarks do not become decorrelated due to hadronization, so their spin information is transferred to their decay products. This makes it possible to measure the top quark pair's spin structure using angular observables of their decay products. In this report we are going to use the 15 observables defined and measured in [10]. These observables are related with the top quark pair's spin density matrix that is presented in section 2.3. In order to measure all observables, the final-state particles of the decay chains of the pair $t\bar{t}$ have to be reconstructed and identified correctly. The top quark decays in almost all cases via electroweak interaction into a b quark and a W boson (the CKM matrix element is $|V_{tb}| = 0.99914 \pm 0.00005$ [1]). The W boson decays either leptonically (to one lepton and one neutrino) or hadronically (to one quark and one antiquark). As charged leptons retain more information about the spin state of the top quarks, and they can be precisely reconstructed, the measurements of these observables were performed in the dileptonic final state (both W decay leptonically, leading to a final state with two quarks, two charged leptons, and two neutrinos). The dileptonic channel offers a pure sample since the background contribution is smaller than in the other channels (fully hadronic or semileptonic).

2.2 Two-Higgs-Doublet model

The two Higgs Doublet Model is a simple extension of SM Higgs, with two complex Higgs field-doublets and five Higgs bosons of spin 0 [14]. Those bosons are h (CP-even, neutral, SM like), H (CP-even, neutral, high mass), A (CP-odd, neutral, high mass), H[±]

and H^- (charged, high mass). This theory has 7 free parameters: m_h , m_A , $m_H = m_{H^+} = m_{H^-}$, the mixing angle α among the neutral Higgs bosons, the ratio of the vacuum expectation values of the two Higgs doublets fields Φ_1 and Φ_2 , $\tan \beta = \nu_1/\nu_2$, and the potential m_{12}^2 of the softly break term.

In this model, the $t\bar{t}$ pair could be produced via the following Feynman diagrams:

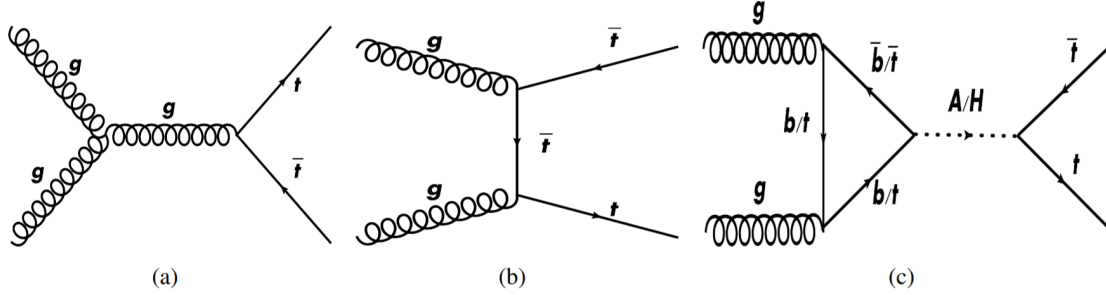


Figure 1: Feynman diagrams for $t\bar{t}$ production in 2HDM.

The usual way to discover those new particles would be to look for a bump in the $t\bar{t}$ pair invariant mass distribution but the interference of the other Feynman diagrams make our measurement less sensitive. Those interferences deform the usual bump that becomes a dip and a bump as we see in Figures 2, 3 and 4. Due to the limited resolution on the $t\bar{t}$ invariant mass, the shape of the signal makes it more difficult to detect as we see in. For this reason, the authors [15] could only exclude a few models in their analysis as we can see in Figure 5 where just the models below the blue line are excluded. For solving this problem, we have to look in other top properties. In this report we will look in the spin polarization and correlation of the top pair. In the next section a set of polarization and spin correlation observables will be presented. We will study the behaviour of these observables in different 2HDM models to try to exclude some of them and constrain their free parameters.

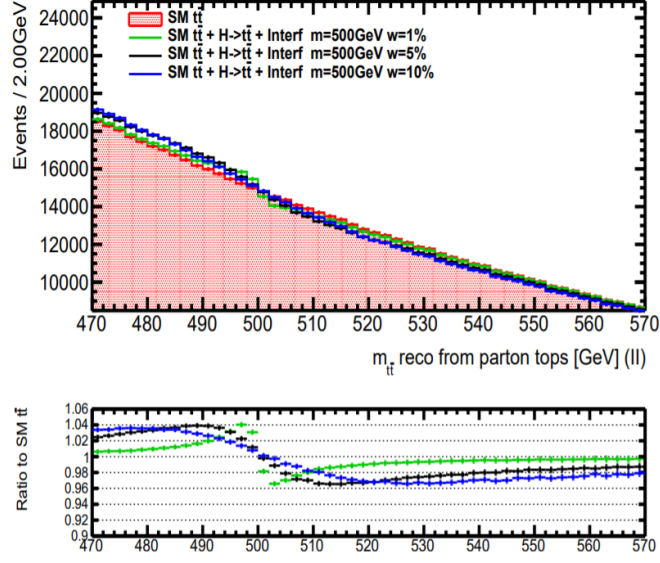


Figure 2: $t\bar{t}$ pair invariant mass distribution for the process $H \rightarrow t\bar{t}$ with $m_H = 500$ GeV overlaid with the signals of different widths (1%, 5% and 10%).

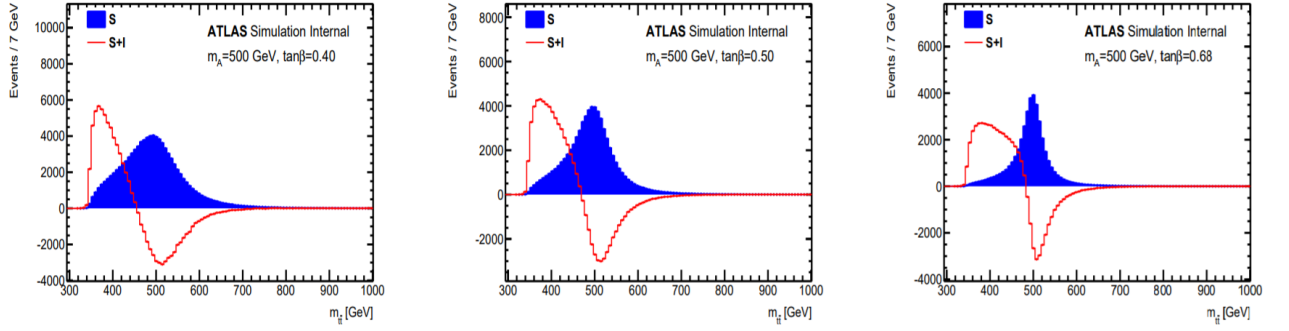


Figure 3: Pure resonance signal (S) and signal+interference (S+I) for $m_{t\bar{t}}$ distributions for $m_A = 500$ GeV.

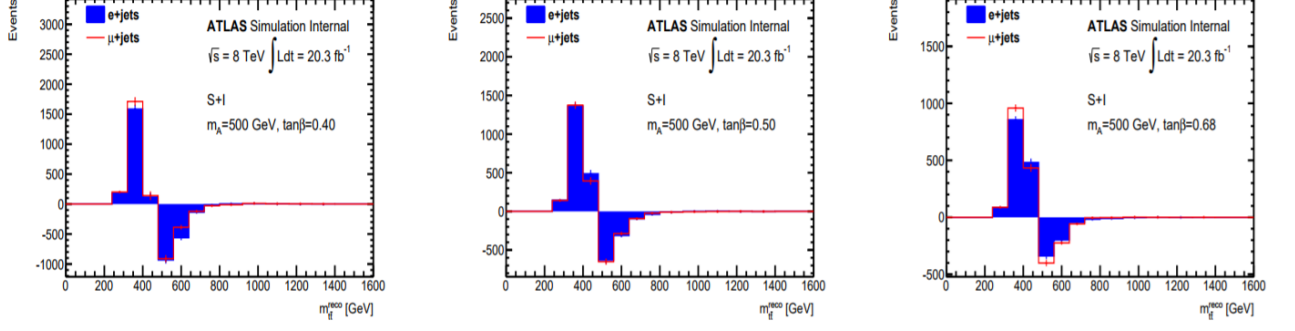


Figure 4: Pure resonance signal (S) and signal+interference (S+I) for $m_{t\bar{t}}$ distributions for $m_A = 500$ GeV at reconstruction level.

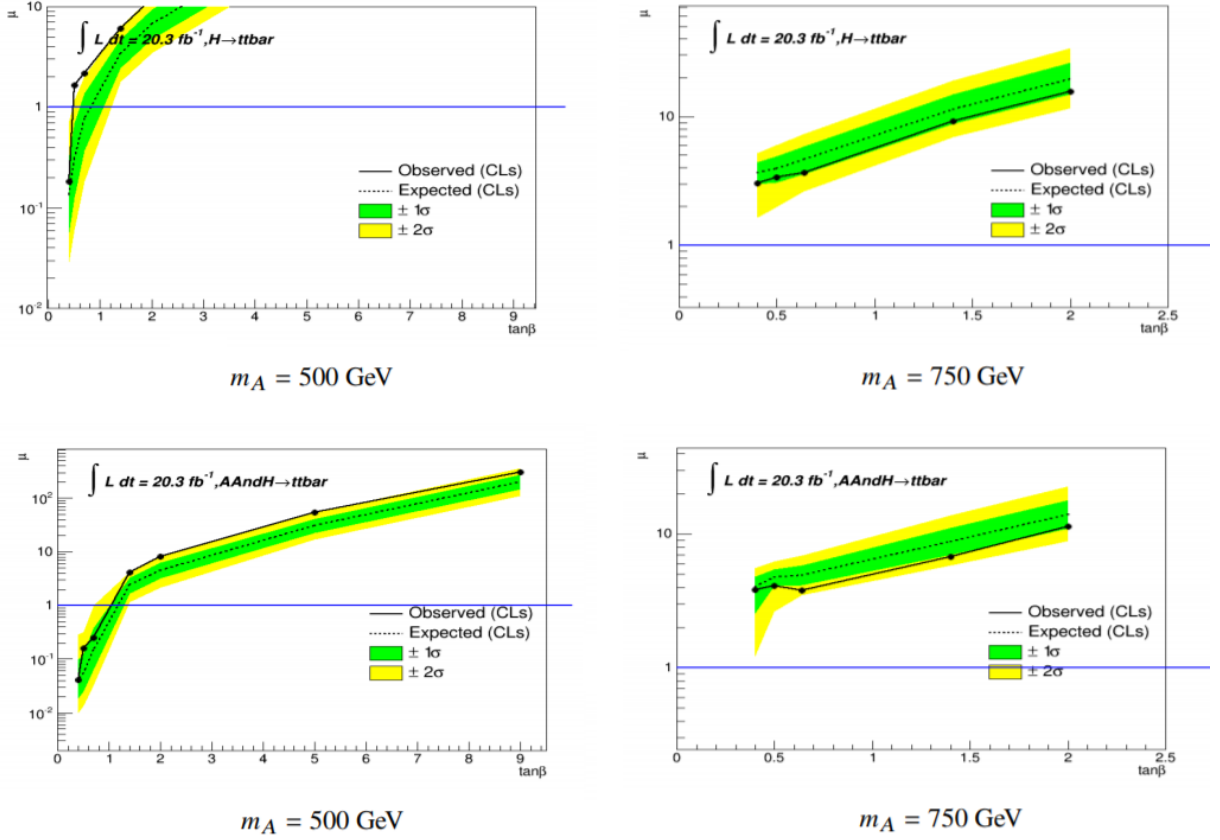


Figure 5: Exclusion plots obtained by [15] using the $t\bar{t}$ invariant mass for the different models that we study in this report. The models below the blue line are excluded.

Several MC simulations have been performed for this model changing the different free parameters for the processes $gg \rightarrow A \rightarrow t\bar{t}$ and $gg \rightarrow H \rightarrow t\bar{t}$ [15]. Table 1 shows the list of ntuples that we use in the data analysis. The parameters of the model that we change

for the comparison with the data and the SM are $\tan \beta$ (between $0.40 - 9.00$), m_A (500 and 750 GeV) and m_H (500 and 750 GeV). The rest of the parameters are known from the SM or we fix them.

2.3 Polarization and spin correlation

The degree of polarization of a particle (P) is the expectation value of the helicity of the particle:

$$P = \langle \vec{S} \cdot \hat{p} \rangle \quad (1)$$

where \vec{S} is the spin of the particle and \hat{p} is a unitary vector in the direction of the momentum of the particle.

The spin correlation (C) can be expressed as the ratio of the difference of spin-aligned pairs and spin anti-aligned pairs in a given frame of reference (spin-quantization axis):

$$C = \frac{N(\uparrow\uparrow) + N(\downarrow\downarrow) - N(\uparrow\downarrow) - N(\downarrow\uparrow)}{N(\uparrow\uparrow) + N(\downarrow\downarrow) + N(\uparrow\downarrow) + N(\downarrow\uparrow)} \quad (2)$$

The squared spin density matrix of $t\bar{t}$ production is defined as:

$$|M|^2 \propto \tilde{A} + \mathbf{B}^+ \cdot \mathbf{s}^+ + \mathbf{B}^- \cdot \mathbf{s}^- + C_{ij} s_{1i} s_{2j} \quad (3)$$

where \tilde{A} fixes the cross section of $t\bar{t}$ production, \mathbf{B}^\pm corresponds to the polarization vectors for the top and antitop quark, \mathbf{s}^\pm denote the spin vectors of those quarks and C_{ij} is the spin correlation matrix [2, 9].

The equation (3) can be rewritten in terms of its angular distributions with respect to the production angles of the leptons which come from the top and antitop quark as:

$$\frac{1}{\sigma} \frac{d^2\sigma}{d\cos\theta_a d\cos\theta_b} = \frac{1}{4} \left(1 + B_+^a \cos\theta_+^a + B_-^b \cos\theta_-^b - C(a, b) \cos\theta_+^a \cos\theta_-^b \right) \quad (4)$$

where B^a , B^b and $C(a, b)$ are the polarization and spin correlation along the spin quantization axes a and b . The angles θ^a and θ^b are the angles between the momentum direction of a top quark decay particle in its parent top quark's rest frame and the axis a or b . The subscript $+(-)$ refers to the top (antitop) quark. From equation (4) one can

Table 1: Signal+interference (S+I) sample parameters, for the pseudoscalar Higgs boson A and the scalar H. The cross-sections are from MadGraph, for the processes $gg \rightarrow A \rightarrow t\bar{t}$ and $gg \rightarrow H \rightarrow t\bar{t}$ in the semileptonic+dileptonic channels, $\sin(\beta - \alpha) = 1$. The samples were simulated in ATLFast-II. Table obtained from [15]

Higgs boson	Mass Higgs boson [GeV]	$\tan \beta$	Γ [GeV]	MG σ S+I [pb]
pseudoscalar A	500	0.40	142.950	0.3449200
		0.50	91.489	0.5227500
		0.68	49.467	0.4777999
		1.40	11.687	0.1620898
		2.00	5.754	0.0805555
		5.00	1.144	0.0037320
		9.00	1.025	-0.0073180
	750	0.40	230.239	0.3462499
		0.50	147.355	0.3590277
		0.70	75.186	0.2546666
		1.40	18.820	0.0775444
		2.00	9.261	0.0383016
scalar H	500	0.40	80.559	0.4141900
		0.50	51.559	0.3286700
		0.70	26.309	0.2068600
		1.40	6.594	0.0630540
		2.00	3.259	0.0328520
		5.00	0.901	0.0049130
		9.00	0.744	0.0016100
	750	0.40	189.642	0.1759333
		0.50	121.373	0.1569277
		0.64	74.083	0.1174666
		1.40	15.506	0.0314588
		2.00	7.637	0.0162188

retrieve the relation (5) for the spin correlation between the axes a and b.

$$C(a, b) = -9 \langle \cos \theta_+^a \cos \theta_-^b \rangle \quad (5)$$

Integrating one of the angles in equation (4) gives the single-differential cross section (6).

$$\frac{1}{\sigma} \frac{d\sigma}{d \cos \theta_a} = \frac{1}{2} (1 + B^a \cos \theta_+^a) \quad (6)$$

From equation (6) one can retrieve the relation:

$$B^a = 3 \langle \cos \theta^a \rangle \quad (7)$$

All the observables are based on $\cos \theta$ where, to define the different θ angles (angles between the direction of the momentum of the decayed lepton and an axis) the following basis is chosen using three orthogonal spin quantization axes:

- The helicity axis (k) is defined as the top quark direction in the $t\bar{t}$ rest frame
- The transverse axis (n) is defined to be transverse to the production plane created by the top quark direction and the beam axis
- The r-axis (r) is an axis orthogonal to the other two axis

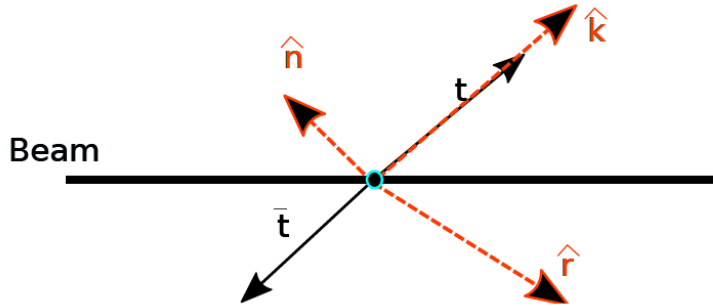


Figure 6: Illustrative drawing of the chosen basis for the top quark decay product.

With this definition of the axes the authors of [9] define a set of observables summarized in Table 2. Each one of the observables is sensitive to one coefficient of the spin density

matrix.

Table 2: The top spin observables, their definitions and their expectation value.

Name	Expectation value	Observable
Helicity polarization	B^k	$\cos \theta_{\pm}^k$
Transverse polarization	B^n	$\cos \theta_{\pm}^n$
R polarization	B^r	$\cos \theta_{\pm}^r$
Helicity correlation	$C(k, k)$	$\cos \theta_{+}^k \cos \theta_{-}^k$
Tranverse correlation	$C(n, n)$	$\cos \theta_{+}^n \cos \theta_{-}^n$
R correlation	$C(r, r)$	$\cos \theta_{+}^r \cos \theta_{-}^r$
R-Hel Sum	$C(r, k) + C(k, r)$	$\cos \theta_{+}^r \cos \theta_{-}^k + \cos \theta_{+}^k \cos \theta_{-}^r$
R-Hel Diff	$C(r, k) - C(k, r)$	$\cos \theta_{+}^r \cos \theta_{-}^k - \cos \theta_{+}^k \cos \theta_{-}^r$
Trans-Hel Sum	$C(n, k) + C(k, n)$	$\cos \theta_{+}^n \cos \theta_{-}^k + \cos \theta_{+}^k \cos \theta_{-}^n$
Trans-Hel Diff	$C(n, k) - C(k, n)$	$\cos \theta_{+}^n \cos \theta_{-}^k - \cos \theta_{+}^k \cos \theta_{-}^n$
Trans-R Sum	$C(n, r) + C(r, n)$	$\cos \theta_{+}^n \cos \theta_{-}^r + \cos \theta_{+}^r \cos \theta_{-}^n$
Trans R-Diff	$C(n, r) - C(r, n)$	$\cos \theta_{+}^n \cos \theta_{-}^r - \cos \theta_{+}^r \cos \theta_{-}^n$

Those observables are not correlated so they are a great tool to test the validity of the SM and to search for theories BSM. In this report we use this observables to study the compatibility between the data and the Two-Higgs-Doublet models (2HDM).

2.4 Chi-squared test with correlations between the bins

In the analysis of the results, we will need to compare the simulated data from the 2HDM with the simulated data from the SM and the real data from ATLAS detector. The χ^2 test is used to compare simulated data and the models. The χ^2 test is given by:

$$\chi^2 = \sum_{j=1}^n \frac{[f(B_j) - f_t(B_j)]^2}{\sigma^2 [f_t(B_j)]} \quad (8)$$

where $f_t(B_j)$ is the theoretical frequency for B_j observed value, $f(B_j)$ is the expected frequency and $\sigma^2 [f_t(B_j)]$ is the variance associated to the B_j value.

In the case the comparison is made between simulations and the ATLAS measurements, the correlations between the different bins is taken into account. Considering this in the χ^2 test we have to use the covariance matrix defined as:

$$V_{ij} = \sigma_i \sigma_j C_{ij} \quad (9)$$

where C_{ij} is the correlation matrix and σ_i is the error associated with bin i .

With this matrix we can calculate the χ^2 using [16].

$$\chi^2 = \Delta^T V^{-1} \Delta \quad (10)$$

where V^{-1} is the inverse of the covariance matrix, and Δ is:

$$\Delta_i = N_{data_i} - N_{model_i} \quad (11)$$

3 Results and discussion

In this report we compare the behaviour of the spin observables defined in the SM [9] and the different 2HDM models of [15] with the measurements performed by ATLAS collaboration in [10]. The purpose of this comparison is trying to find any deviation between the data and the 2HDM in order to find new physics BSM or to discard some of the 2HDM, limiting the possible values of their free parameters.

For constructing the observables we use the MC simulations of the Table 1 and the SM, we reconstructed the dileptonic decay of the $t\bar{t}$ system and the spin quantization axes defined in section 2.2. With this information, we calculated the 15 spin correlation and polarization observables for each event.

3.1 Compatibility between the SM and the 2HDM

First of all, we compare the behaviour of this observables between the SM and the different 2HDM to check if, with enough accuracy, we could distinguish them. An example of this comparison for the 15 observables is shown in Figures 7, 8 and 9. In Table 3 is shown a compilation of the probability of coincidence using the χ^2 test between the SM and each of the 2HDM that we study.

In results shown in Table 3 we can observe that, for all the 2HDM, there are some observables (like the correlations) that are incompatible with the SM for each 2HDM. Other observables show incompatibilities just for some of them (like the polarizations). If enough accuracy is reached in the measured data, it would be possible to distinguish between the SM and the 2HDM with the corresponding parameters. To compare the compatible observables we should increase the amount of MC data until we can distinguish the two models and then, we would compare with the data.

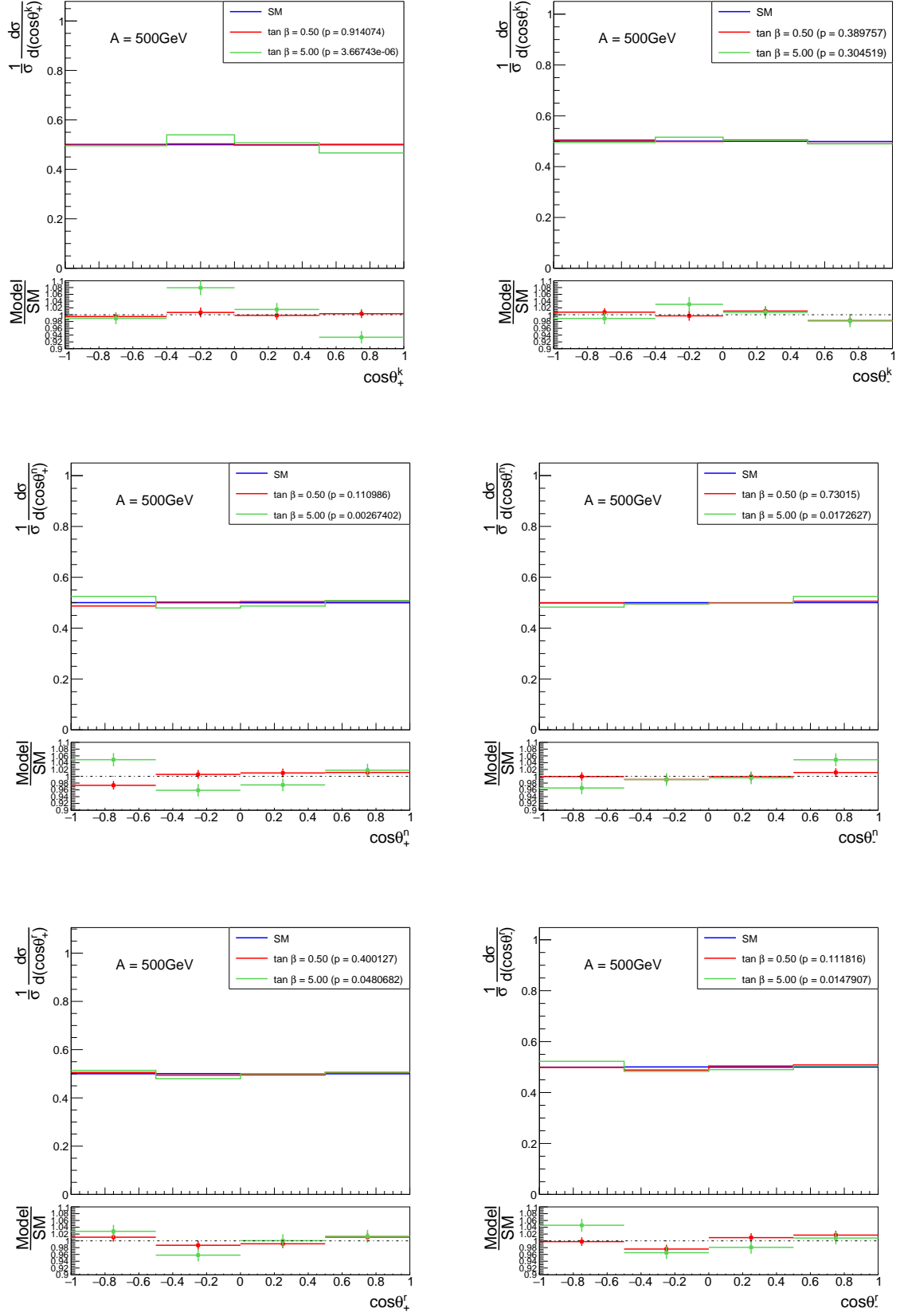


Figure 7: Comparison between SM and two 2HDM MC simulations for the observables $\cos \theta_{\pm}^k$, $\cos \theta_{\pm}^n$ and $\cos \theta_{\pm}^r$. Those 2HDM are for $\tan \beta = 0.50$ and $\tan \beta = 5.00$ corresponding to models with a pseudoscalar Higgs boson A of mass 500 GeV.

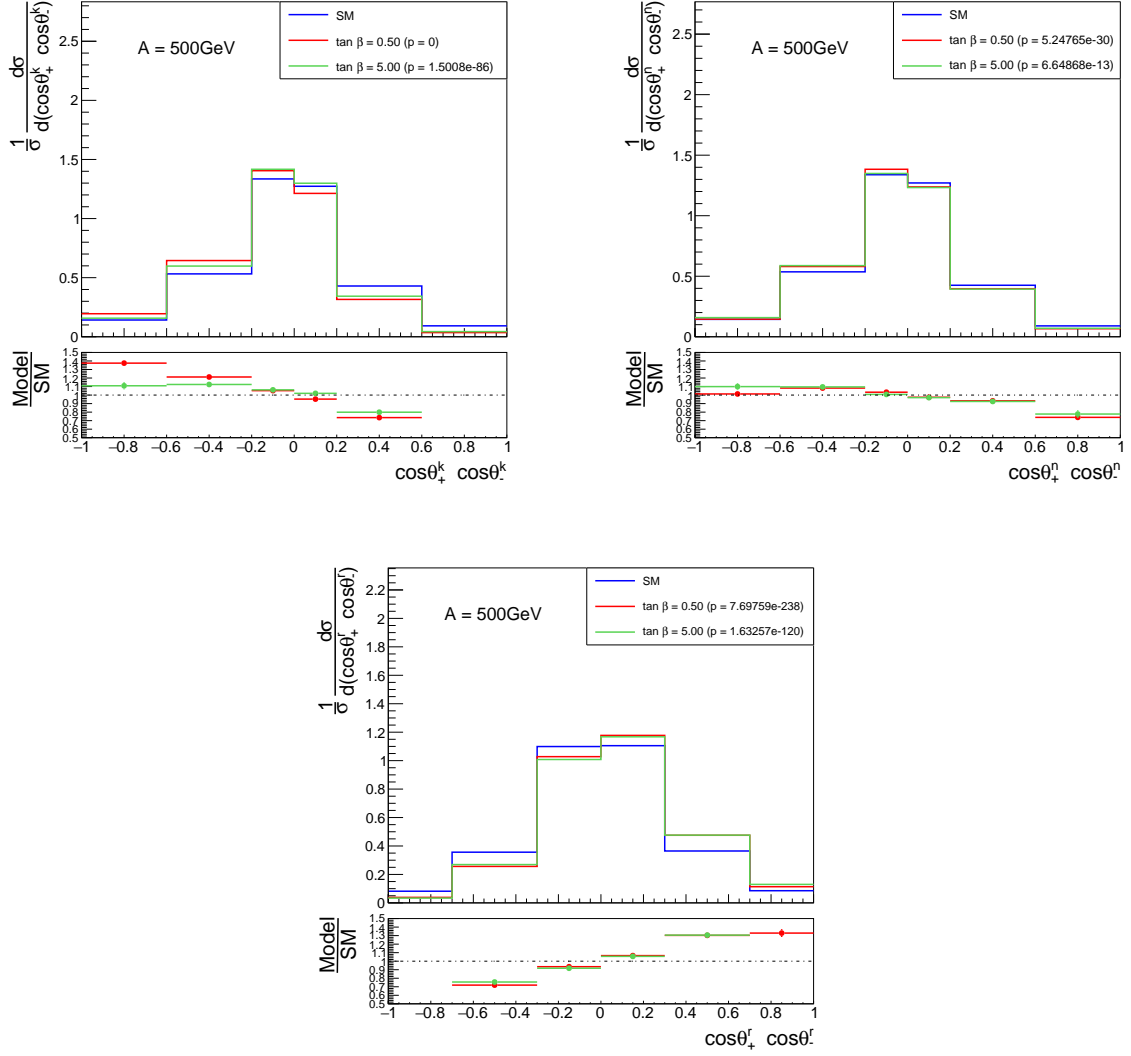


Figure 8: Comparison between SM and two 2HDM MC simulations for the observables $\cos \theta_+^k \cos \theta_-^k$, $\cos \theta_+^n \cos \theta_-^n$ and $\cos \theta_+^r \cos \theta_-^r$. Those 2HDM are for $\tan \beta = 0.50$ and $\tan \beta = 5.00$ corresponding to models with a pseudoscalar Higgs boson A of mass 500 GeV.

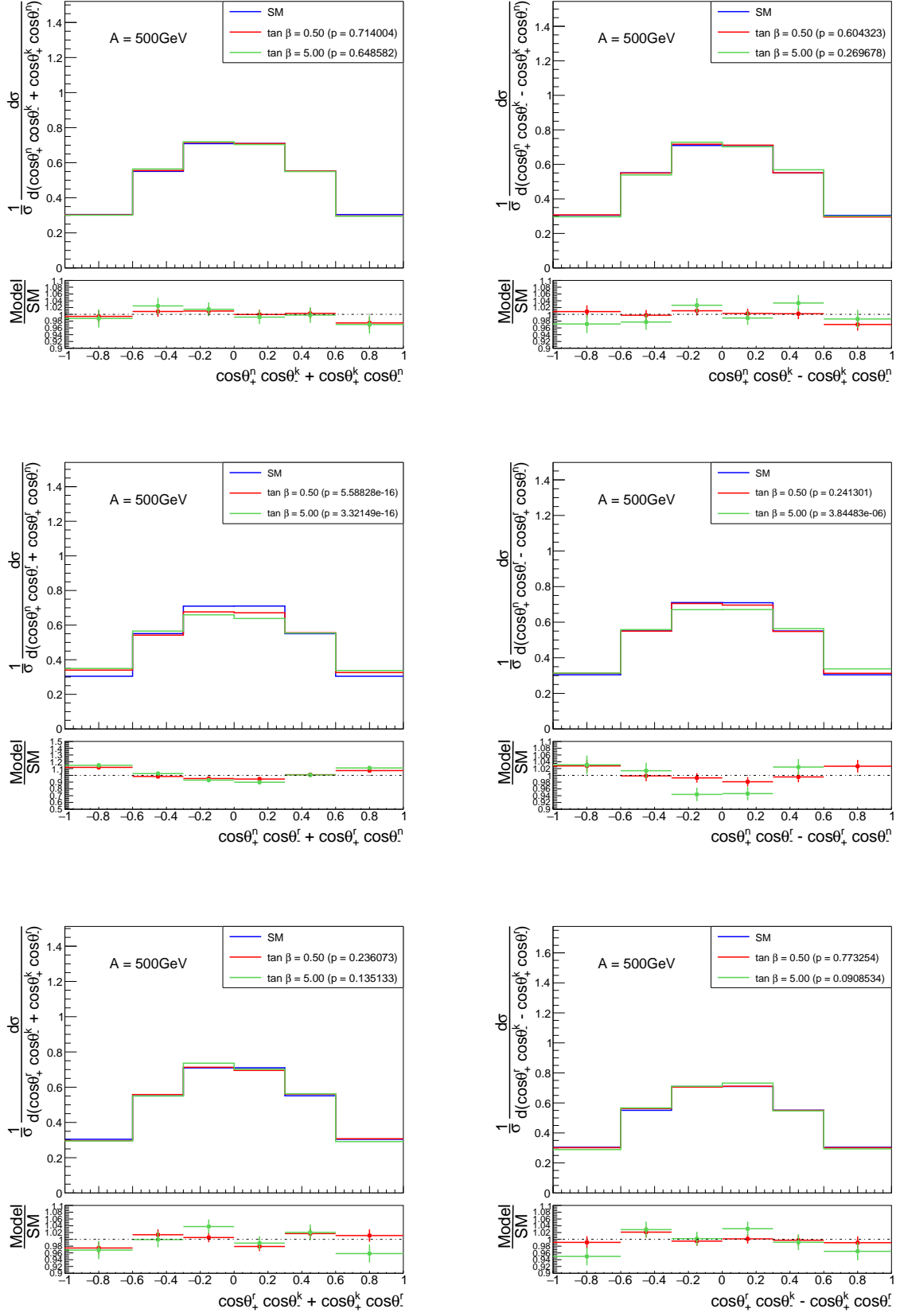


Figure 9: Comparison between SM and two 2HDM MC simulations for the observables $\cos \theta_+^r \cos \theta_-^k + \cos \theta_+^k \cos \theta_-^r$, $\cos \theta_+^r \cos \theta_-^k - \cos \theta_+^k \cos \theta_-^r$, $\cos \theta_+^n \cos \theta_-^k + \cos \theta_+^k \cos \theta_-^n$, $\cos \theta_+^n \cos \theta_-^k - \cos \theta_+^k \cos \theta_-^n$, $\cos \theta_+^r \cos \theta_-^r + \cos \theta_+^r \cos \theta_-^n$ and $\cos \theta_+^n \cos \theta_-^r - \cos \theta_+^r \cos \theta_-^n$. Those 2HDM are for $\tan \beta = 0.50$ and $\tan \beta = 5.00$ corresponding to models with a pseudoscalar Higgs boson A of mass 500 GeV.

3.2 Compatibility between the ATLAS data and the different models

Once we know the observables for which we can distinguish each model from SM, we compare the MC simulations with the measured data from ATLAS [10]. An example of this comparison for some of the observables is shown in Figure 10. In those plots we can see that some observables have more discrepancy between the 2HDM and the data than others. For example, the observables $\cos \theta_+^k$ and $\cos \theta_+^n \cos \theta_-^r + \cos \theta_+^r \cos \theta_-^n$ do not let us exclude this model because, in the first case, the behaviour is really similar and, in the second, the error bars are too big. However, the observable $\cos \theta_+^r \cos \theta_-^r$ show a great discrepancy between the model and the measurement. With a more detailed analysis, we could exclude this model.

Performing these comparisons for more 2HDM and observables we have found several plots which show sensitivity between the SM, the 2HDM distributions and the data (e.g. Figure 11).

In Table 4 is shown a compilation of the probability of coincidence using the χ^2 test without considering correlations between the ATLAS data and different models (all the 2HDM that we study and the SM). In this table we can see that, the more sensitive observables are the correlation $\cos \theta_+^k \cos \theta_-^k$, $\cos \theta_+^n \cos \theta_-^n$ and $\cos \theta_+^r \cos \theta_-^r$.

In Table 5 is shown the same compilation of the probability of coincidence but, this time, using the χ^2 test taking into account the correlations (as we studied in section 2.4). Comparing these tables (with and without correlation) we can see that, in general, the correlation between the bins decrease the probability of coincidence.

Although a more detailed analysis has to be performed, we have several evidences of models that we could exclude that the usual method described in section 2.2 could not (e.g. Figure 12).

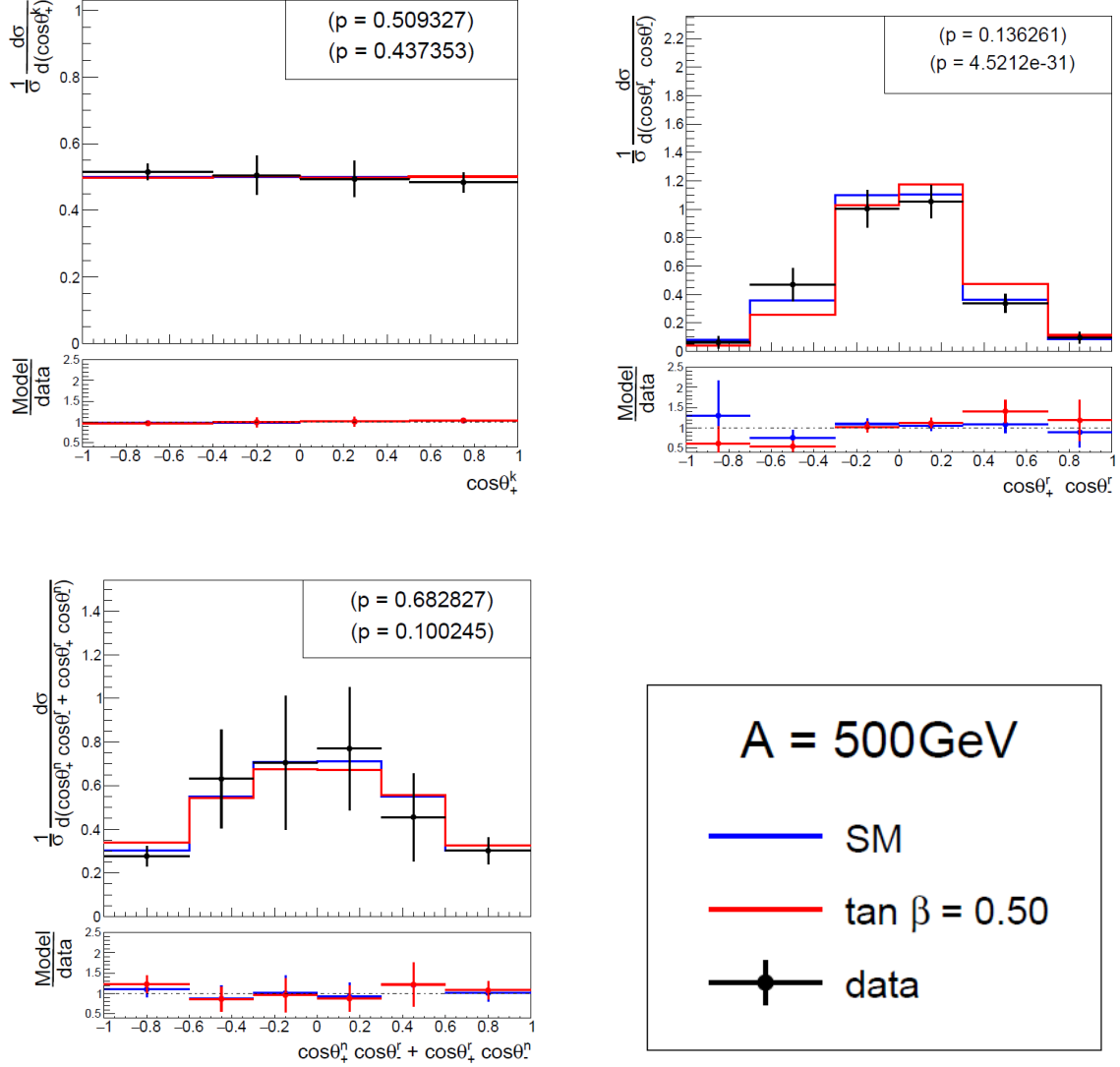


Figure 10: Example of plots for each kind of observable comparing the SM, one 2HDM with $m_A = 500$ GeV and $\tan \beta = 0.50$ and the ATLAS data. The probability of coincidence have been calculated using the χ^2 test considering correlations (as shown in section 2.4).

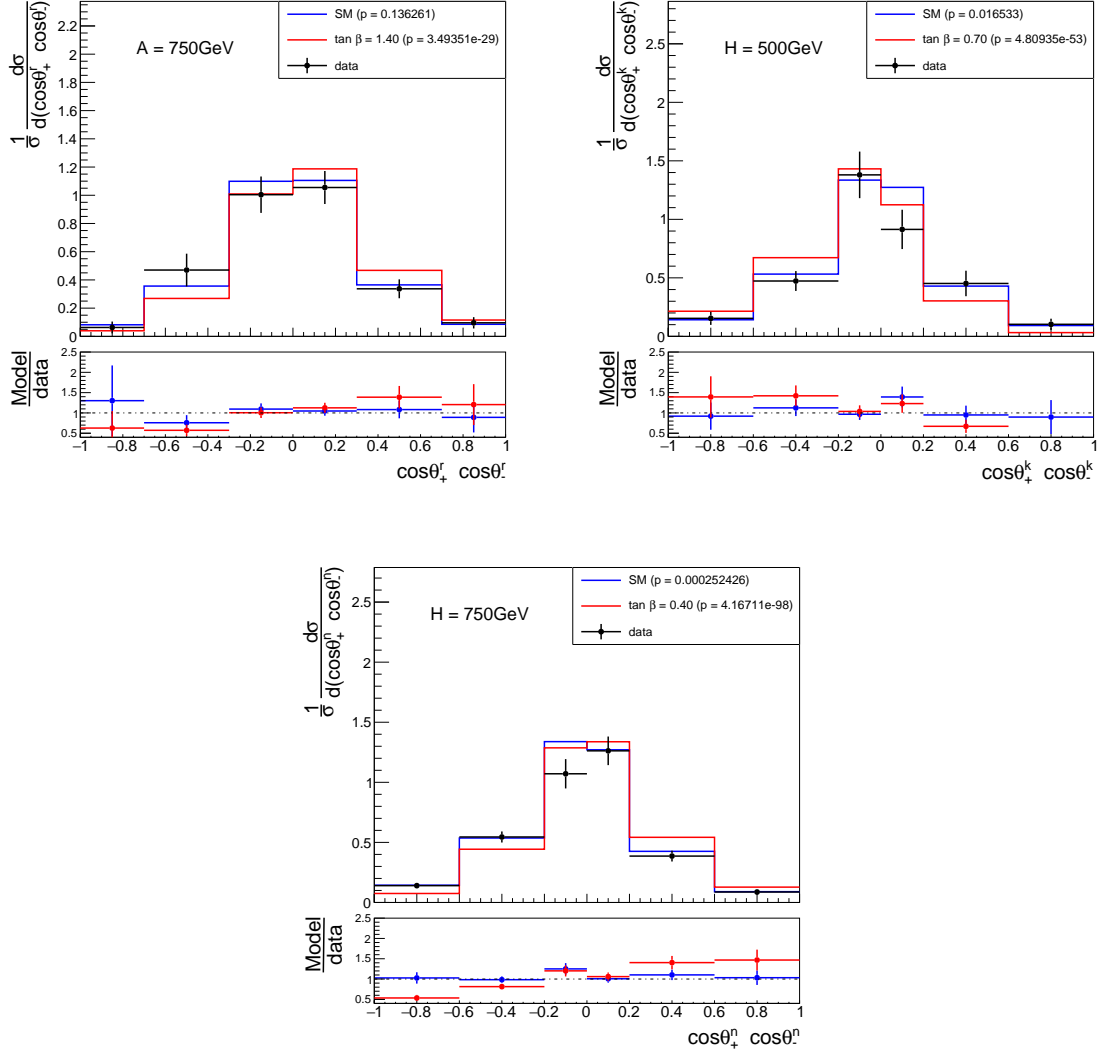


Figure 11: Comparison between different 2HDM and the ATLAS data for some polarization observables.

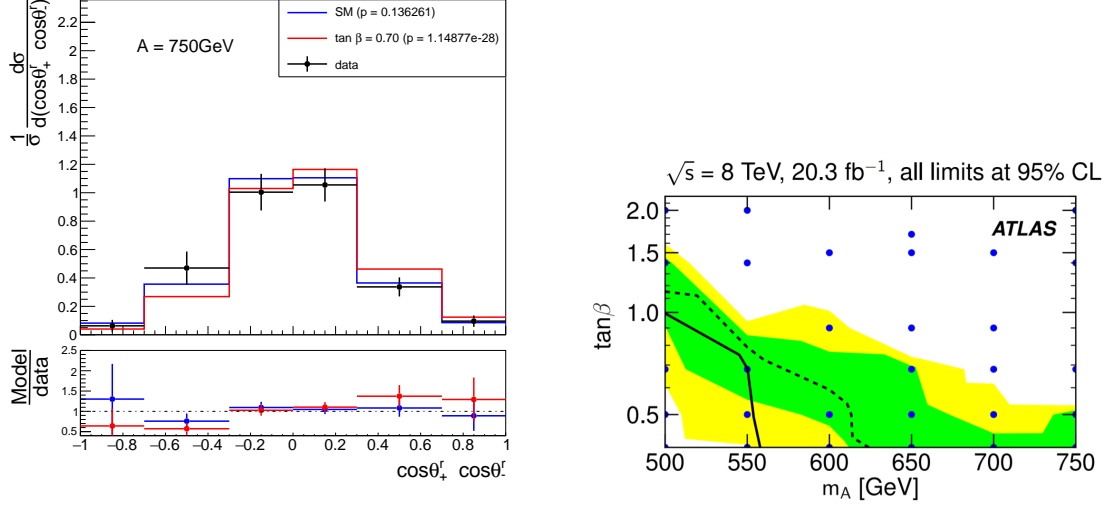


Figure 12: Left: comparison between the ATLAS data and the 2HDM with $m_A = 750$ GeV and $\tan\beta = 0.70$ for the observable $\cos\theta_+^r \cos\theta_-^r$. Right: exclusion plot from [15] for the pseudoescalar A.

4 Conclusions

Many theories have been proposed to solve the limitations of the Standard Model. The techniques used for this finality are diverse. In many of them, the top quark plays an important role due to its great mass which might mean that he would play a special role with BSM particles. If supermassive particles exist, they would probably decay to top quark (or to $t\bar{t}$ pair). In this project, we have worked with a simple extension of the SM Higgs, the 2HDM. This model proposes five Higgs boson and two of them contribute to the production of $t\bar{t}$ pairs via the Feynman diagram of Figure 1. We have also seen that the authors of [9] tried to use the invariant mass of $t\bar{t}$ pair to find this particles but, the interference between Feynman diagrams caused the measurements to be less sensitive, reason for which we were able to exclude only a few values of the free model parameters. This difficulty in finding particles has encouraged to study others properties of top quark, in our case, the polarization and the spin correlation of the $t\bar{t}$ pair. In [15] the authors used a set of observables, described in Section 2.2, and they compared with the SM without observing any significative discrepancy. In this work, we have compared the behaviour of these observables in different 2HDM, seeing that we can always find some observable which differs with SM and allows us to distinguish it from SM. Then, we performed the same comparison in [9], but, in this case, we compared the ATLAS data with the results obtained from reconstructing the observables for the MC simulations of 2HDM.

The results we obtained from doing these comparisons are very promising, since we observed significative discrepancies between measured values and the predicted by lots of

2HDM. The different preliminary statistical analysis we have performed point out that, in general, the correlations are the observables which are most sensitive because their measurements have relatively small associated errors. If we examine the results provided by the χ^2 test, without considering the correlations, we see that the biggest discrepancies we can find in the observable $\cos \theta_+^n \cos \theta_-^n$ for all 2HDM with the scalar H. Also, we observe a significative discrepancy in the observable $\cos \theta_-^k$ in the model with $m_A = 500$ y $\tan \beta = 9.00$.

Performing a more complete statistical test (χ^2 with correlations), as we showed in Section 2.4, we noted some results with a higher discrepancy between 2HDM and data. This is because, in general, the correlations tended to move the data away from the models prediction. The biggest discrepancies are still observed in the observables related with the correlations ($\cos \theta_+^k \cos \theta_-^k$, $\cos \theta_+^n \cos \theta_-^n$, $\cos \theta_+^r \cos \theta_-^r$).

This is the first attempt to interpret the measurement of the top spin observables to constrain new physics models. Results seem very promising but are still very preliminary. More studies are needed to understand the sensitivity of the observables and optimize the interpretation. For example, we have consider that the correlation affects at all the error bar of the data but, in fact, it does not affect to the modeling uncertainty. This could lead to very interesting results in terms of interpretation of precise top quark properties.

Table 3: Probability of coincidence between the MC data obtained using the SM and the different 2HDM [15] for the 15 observables defined in [9]. The comparison have been performed using the χ^2 test. Probabilities under 10^{-10} (inclusive) have been considered to be zero.

Mass A [GeV]	500						750							
Observables	$\tan \beta$		0.40	0.50	0.68	1.40	2.00	5.00	9.00	0.40	0.50	0.70	1.40	2.00
$\cos \theta_+^k$	0.547	0.914	0.00253	0.00335	0.0416	$3.67 \cdot 10^{-6}$	0	$4.48 \cdot 10^{-5}$	0.000121	$2.95 \cdot 10^{-7}$	$1.29 \cdot 10^{-5}$	$1.69 \cdot 10^{-9}$		
$\cos \theta_-^k$	0.420	0.390	0.932	0.000188	0.0363	0.305	0	$7.90 \cdot 10^{-9}$	$1.31 \cdot 10^{-5}$	0.000181	$4.60 \cdot 10^{-9}$	$7.03 \cdot 10^{-8}$		
$\cos \theta_+^n$	0.0672	0.111	0.901	0.765	0.226	0.00267	0	0.0736	0.0143	0.000277	0.000211	0.000239		
$\cos \theta_-^n$	0.731	0.730	0.293	0.0884	0.630	0.0173	0	0.0237	0.0200	0.556	0.00294	0.000175		
$\cos \theta_+^r$	0.850	0.400	0.134	0.8253	0.189	0.0481	0	0.00676	0.082	0.0161	0.000122	0.00511		
$\cos \theta_-^r$	0.888	0.112	0.845	0.00685	0.0443	0.0148	0	0.000816	0.000363	0.226	0.0595	0.0100		
$\cos \theta_+^k \cos \theta_-^k$	0	0	0	0	0	0	0	0	0	0	0	0		
$\cos \theta_+^k \cos \theta_-^n$	0	0	0	0	0	0	0	0	0	0	0	0		
$\cos \theta_+^k \cos \theta_-^r$	0	0	0	0	0	0	0	0	0	0	0	0		
$\cos \theta_+^r \cos \theta_-^k + \cos \theta_+^k \cos \theta_-^r$	0.396	0.236	0.753	0.764	0.917	0.135	0	0.0133	0.000211	0.175	0.0264	0.0149		
$\cos \theta_+^r \cos \theta_-^k - \cos \theta_+^k \cos \theta_-^r$	0.769	0.773	0.503	0.227	0.106	0.0909	0	0.000720	0.0770	$1.73 \cdot 10^{-5}$	0.213	0.000125		
$\cos \theta_+^n \cos \theta_-^k + \cos \theta_+^k \cos \theta_-^n$	0.942	0.714	0.225	0.0721	0.192	0.649	0	0.00842	0.00527	0.000424	0.00678	0.0457		
$\cos \theta_+^n \cos \theta_-^k - \cos \theta_+^k \cos \theta_-^n$	0.115	0.604	0.877	0.676	0.103	0.270	0	0.00363	0.514	0.0154	$2.96 \cdot 10^{-6}$	0.0907		
$\cos \theta_+^r \cos \theta_-^k + \cos \theta_+^k \cos \theta_-^r$	$1.46 \cdot 10^{-6}$	0	$4.38 \cdot 10^{-7}$	$1.60 \cdot 10^{-8}$	0	0	0	0	0	0	0	0		
$\cos \theta_+^r \cos \theta_-^k - \cos \theta_+^k \cos \theta_-^r$	0.811	0.241	0.271	0.0499	0.00942	$3.84 \cdot 10^{-6}$	0	$9.24 \cdot 10^{-7}$	0.000603	$1.23 \cdot 10^{-8}$	0	0		

Mass H [GeV]		500						750					
tan β		0.40	0.50	0.68	1.40	2.00	5.00	9.00	0.40	0.50	0.64	1.40	2.00
Observables	$\cos \theta_+^k$	$1.29 \cdot 10^{-5}$	0.000146	0.00723	$8.22 \cdot 10^{-7}$	0.00338	0.00101	0.443	0.00978	0.425	0.392	0.2667	0.0750
	$\cos \theta_-^k$	$9.93 \cdot 10^{-5}$	0.0475	0.0969	$2.29 \cdot 10^{-6}$	0.0357	0.00956	0.0321	0.129	0.744	0.0805	0.692	0.570
	$\cos \theta_+^n$	0.0120	0.429	0.0870	0.0224	0.244	0.0178	0.0145	0.0145	0.495	0.385	0.237	0.00583
	$\cos \theta_-^n$	0.124	0.276	0.243	0.206	0.325	0.194	0.186	0.186	0.920	0.279	0.0112	0.259
	$\cos \theta_+^r$	0.386	0.676	0.0259	0.0950	0.126	0.150	0.802	0.802	0.462	0.486	0.618	0.286
	$\cos \theta_-^r$	0.0165	0.268	0.0998	0.039	0.935	0.673	0.172	0.172	0.107	0.112	0.960	0.236
	$\cos \theta_+^k \cos \theta_-^k$	0	0	0	0	0	0	0	0	0	0	0	0
	$\cos \theta_+^n \cos \theta_-^n$	0	0	0	0	0	0	0	0	0	0	0	0
	$\cos \theta_+^r \cos \theta_-^r$	0	0	0	0	0	0	0	0	0	0	0	0
	$\cos \theta_+^r \cos \theta_-^k + \cos \theta_+^k \cos \theta_-^r$	0.0315	0.145	0.642	0.0307	0.478	0.327	0.183	0.183	0.00939	0.100	0.322	0.00190
$\cos \theta_+^r \cos \theta_-^k - \cos \theta_+^k \cos \theta_-^r$	$3.26 \cdot 10^{-5}$	$4.39 \cdot 10^{-7}$	0.00146	$1.16 \cdot 10^{-7}$	$1.00 \cdot 10^{-6}$	$5.41 \cdot 10^{-9}$	$8.41 \cdot 10^{-9}$	$8.41 \cdot 10^{-9}$	0.138	0.0318	0.323	$9.82 \cdot 10^{-5}$	0.0222
$\cos \theta_+^n \cos \theta_-^k + \cos \theta_+^k \cos \theta_-^n$	0.00695	0.0716	$4.41 \cdot 10^{-6}$	$3.61 \cdot 10^{-6}$	0.00020271	0.000732	0.000128	0.000128	0.574	0.772	0.213	0.125	$3.81 \cdot 10^{-5}$
$\cos \theta_+^n \cos \theta_-^k - \cos \theta_+^k \cos \theta_-^n$	0.330	0.00251	0.176	0.00562	0.0840	0.371	0.723	0.723	0.274	0.384	0.478	0.793	0.405
$\cos \theta_+^r \cos \theta_-^r + \cos \theta_+^r \cos \theta_-^n$	0.000269	$6.81 \cdot 10^{-5}$	0.00584	0.444	0.577	0.0343	$1.14 \cdot 10^{-10}$	$1.14 \cdot 10^{-10}$	0	0	0	0	0
$\cos \theta_+^r \cos \theta_-^r - \cos \theta_+^r \cos \theta_-^n$	$6.03 \cdot 10^{-5}$	0.206	0.000537	$6.76 \cdot 10^{-5}$	0.0519	0.0275	0.00399	0.00399	0.476	0.130	0.496	0.807	0.561

Table 4: Probability of coincidence between the measured data from ATLAS detector [10] and the MC data from the different models (SM and 2HDM [15]) for the 15 observables defined in [9]. The comparison have been performed using a χ^2 test. Probabilities under 10^{-10} have been considered to be zero.

Mass A [GeV]		500						750						
$\tan \beta$		SM	0.40	0.50	0.68	1.40	2.00	5.00	9.00	0.40	0.50	0.70	1.40	2.00
Observables														
$\cos \theta_+^k$		0.887	0.856	0.851	0.729	0.941	0.939	0.686	0.038	0.790	0.738	0.693	0.719	0.503
$\cos \theta_-^k$		0.665	0.817	0.679	0.629	0.483	0.514	0.610	$6.14 \cdot 10^{-3}$	0.389	0.309	0.537	0.359	0.351
$\cos \theta_+^n$		0.970	0.969	0.936	0.959	0.955	0.921	0.728	0.533	0.932	0.872	0.803	0.800	0.796
$\cos \theta_-^n$		0.888	0.887	0.851	0.813	0.701	0.789	0.578	0.034	0.647	0.604	0.841	0.530	0.453
$\cos \theta_+^r$		0.401	0.361	0.380	0.430	0.361	0.447	0.243	0.177	0.324	0.292	0.259	0.296	0.332
$\cos \theta_-^r$		0.909	0.941	0.971	0.939	0.832	0.875	0.841	0.594	0.940	0.863	0.907	0.898	0.842
$\cos \theta_+^k \cos \theta_-^k$		0.622	0.175	0.158	0.139	0.175	0.165	0.247	0.147	0.218	0.221	0.205	0.204	0.237
$\cos \theta_+^n \cos \theta_-^n$		0.562	0.328	0.213	0.144	0.028	0.0309	0.357	0.455	0.378	0.312	0.202	0.237	0.350
$\cos \theta_+^r \cos \theta_-^r$		0.876	0.155	0.136	0.130	0.130	0.092	0.129	0.611	0.238	0.154	0.194	0.169	0.202
$\cos \theta_+^n \cos \theta_-^k + \cos \theta_+^k \cos \theta_-^n$		0.646	0.695	0.722	0.647	0.681	0.676	0.733	0.65	0.679	0.734	0.729	0.696	0.718
$\cos \theta_+^r \cos \theta_-^k - \cos \theta_+^k \cos \theta_-^r$		0.946	0.947	0.944	0.942	0.947	0.915	0.940	0.862	0.927	0.929	0.914	0.925	0.915
$\cos \theta_+^n \cos \theta_-^k + \cos \theta_+^k \cos \theta_-^n$		0.860	0.873	0.853	0.824	0.852	0.818	0.836	0.580	0.775	0.804	0.723	0.792	0.770
$\cos \theta_+^n \cos \theta_-^k - \cos \theta_+^k \cos \theta_-^n$		0.995	0.995	0.990	0.993	0.997	0.997	0.995	0.965	0.999	0.994	0.999	0.995	0.997
$\cos \theta_+^n \cos \theta_-^r + \cos \theta_+^r \cos \theta_-^n$		0.980	0.875	0.750	0.872	0.860	0.868	0.621	0.000611	0.381	0.474	0.419	0.389	0.307
$\cos \theta_+^n \cos \theta_-^r - \cos \theta_+^r \cos \theta_-^n$		0.805	0.890	0.788	0.804	0.761	0.779	0.826	0.146	0.755	0.730	0.542	0.688	0.691

Mass H [GeV]	500								750			
$\tan \beta$	0.40	0.50	0.68	1.40	2.00	5.00	9.00	0.40	0.50	0.64	1.40	2.00
Observables												
$\cos \theta_+^k$	0.718	0.860	0.803	0.803	0.827	0.826	0.864	0.878	0.968	0.895	0.939	0.951
$\cos \theta_-^k$	0.698	0.608	0.805	0.765	0.833	0.817	0.844	0.761	0.715	0.665	0.694	0.789
$\cos \theta_+^n$	0.917	0.980	0.921	0.875	0.941	0.989	0.884	0.940	0.951	0.926	0.972	0.822
$\cos \theta_-^n$	0.957	0.977	0.967	0.887	0.877	0.968	0.829	0.933	0.785	0.601	0.950	0.743
$\cos \theta_+^r$	0.459	0.384	0.336	0.389	0.485	0.533	0.453	0.389	0.324	0.370	0.273	0.494
$\cos \theta_-^r$	0.844	0.834	0.892	0.872	0.925	0.935	0.886	0.842	0.898	0.928	0.817	0.878
$\cos \theta_+^k \cos \theta_-^k$	0.075	0.079	0.109	0.065	0.101	0.098	0.106	0.157	0.187	0.160	0.182	0.149
$\cos \theta_+^n \cos \theta_-^n$	$7.51 \cdot 10^{-7}$	$1.24 \cdot 10^{-7}$	$3.00 \cdot 10^{-8}$	$7.91 \cdot 10^{-9}$	0	$2.903 \cdot 10^{-9}$	0	$2.99 \cdot 10^{-6}$	$1.24 \cdot 10^{-6}$	$4.59 \cdot 10^{-7}$	$2.38 \cdot 10^{-7}$	$3.40 \cdot 10^{-7}$
$\cos \theta_+^r \cos \theta_-^r$	0.613	0.579	0.538	0.483	0.489	0.447	0.377	0.716	0.697	0.712	0.592	0.617
$\cos \theta_+^n \cos \theta_-^k + \cos \theta_+^k \cos \theta_-^n$	0.605	0.640	0.679	0.621	0.696	0.682	0.545	0.763	0.719	0.654	0.734	0.728
$\cos \theta_+^n \cos \theta_-^k - \cos \theta_+^k \cos \theta_-^n$	0.943	0.927	0.957	0.912	0.956	0.936	0.952	0.959	0.937	0.937	0.943	0.924
$\cos \theta_+^r \cos \theta_-^k + \cos \theta_+^k \cos \theta_-^r$	0.903	0.866	0.911	0.908	0.891	0.896	0.918	0.843	0.862	0.881	0.911	0.941
$\cos \theta_+^r \cos \theta_-^k - \cos \theta_+^k \cos \theta_-^r$	0.995	0.991	0.986	0.954	0.995	0.999	0.995	0.998	0.998	0.996	0.998	0.990
$\cos \theta_+^n \cos \theta_-^r + \cos \theta_+^r \cos \theta_-^n$	0.929	0.907	0.950	0.984	0.980	0.996	0.982	0.383	0.633	0.668	0.757	0.696
$\cos \theta_+^n \cos \theta_-^r - \cos \theta_+^r \cos \theta_-^n$	0.713	0.788	0.749	0.723	0.901	0.792	0.833	0.875	0.752	0.855	0.790	0.826

Table 5: Probability of coincidence between the measured data from ATLAS detector [10] and the MC data from the different models (SM and 2HDM [15]) for the 15 observables defined in [9]. The comparison have been performed using a χ^2 test with correlation. Probabilities under 10^{-10} have been considered to be zero.

Mass A [GeV]		500							750						
Observables	$\tan \beta$	SM													
		0.40	0.50	0.68	1.40	2.00	5.00	9.00	0.40	0.50	0.64	0.70	1.40	2.00	
$\cos \theta_+^k$		0.509	0.508	0.437	0.366	0.836	0.726	0.387	0.00142	0.501	0.433	0.379	0.371	0.149	
$\cos \theta_-^k$		0.105	0.356	0.194	0.083	0.126	0.0667	0.119	$2.015 \cdot 10^{-6}$	0.0955	0.0131	0.135	0.0377	0.0317	
$\cos \theta_+^n$		0.884	0.953	0.393	0.756	0.900	0.616	0.472	0.227	0.841	0.684	0.598	0.626	0.457	
$\cos \theta_-^n$		0.565	0.665	0.559	0.381	0.339	0.334	0.298	$6.23 \cdot 10^{-5}$	0.104	0.0686	0.457	0.116	0.0230	
$\cos \theta_+^r$		0.298	0.240	0.271	0.295	0.212	0.334	0.155	0.0392	0.0780	0.184	0.112	0.208	0.199	
$\cos \theta_-^r$		0.618	0.746	0.929	0.753	0.421	0.638	0.298	0.173	0.587	0.628	0.7286	0.536	0.547	
$\cos \theta_+^k \cos \theta_-^k$		0.0165	0	0	0	0	0	0	$2.39 \cdot 10^{-5}$	0	0	0	0	0	
$\cos \theta_+^n \cos \theta_-^n$		0.0002520	$6.15 \cdot 10^{-6}$	0	0	0	0	0	0	0	0	0	0	0	
$\cos \theta_+^r \cos \theta_-^r$		0.136	0	0	0	0	0	0	0	0	0	0	0	0	
$\cos \theta_+^k \cos \theta_-^k + \cos \theta_+^n \cos \theta_-^n$		0.0559	0.0385	0.106	0.0378	0.0756	0.0697	0.0431	0.00138	0.0186	0.0272	0.0679	0.126	0.0561	
$\cos \theta_+^k \cos \theta_-^k - \cos \theta_+^n \cos \theta_-^n$		0.675	0.685	0.660	0.613	0.709	0.554	0.682	0.427	0.550	0.6220	0.521	0.644	0.703	
$\cos \theta_+^n \cos \theta_-^n + \cos \theta_+^k \cos \theta_-^k$		0.292	0.281	0.211	0.217	0.199	0.178	0.161	0.0136	0.144	0.142	0.0997	0.120	0.125	
$\cos \theta_+^n \cos \theta_-^n - \cos \theta_+^k \cos \theta_-^k$		0.959	0.814	0.903	0.892	0.993	0.9996	0.998	0.536	0.997	0.881	0.999	0.995	0.997	
$\cos \theta_+^r \cos \theta_-^r + \cos \theta_+^k \cos \theta_-^k$		0.683	0.295	0.100	0.227	0.250	0.181	0.017	0	0.000286	0.00211	0.000763	0.000377	$2.31 \cdot 10^{-5}$	
$\cos \theta_+^r \cos \theta_-^r - \cos \theta_+^k \cos \theta_-^k$		0.805	0.837	0.827	0.808	0.786	0.7901	0.440	0.000575	0.674	0.708	0.403	0.413	0.447	

Mass H [GeV]		500							750						
Observables	$\tan \beta$	0.40													
		0.50	0.68	1.40	2.00	5.00	9.00	0.40	0.50	0.64	0.70	1.40	2.00		
$\cos \theta_+^k$		0.250	0.579	0.245	0.456	0.306	0.469	0.396	0.714	0.779	0.640	0.662	0.830		
$\cos \theta_-^k$		0.0943	0.0242	0.308	0.102	0.242	0.166	0.270	0.359	0.192	0.207	0.183	0.291		
$\cos \theta_+^n$		0.863	0.958	0.612	0.908	0.812	0.921	0.891	0.735	0.511	0.434	0.852	0.262		
$\cos \theta_-^n$		0.712	0.913	0.795	0.376	0.367	0.920	0.240	0.716	0.408	0.240	0.809	0.362		
$\cos \theta_+^r$		0.261	0.324	0.220	0.212	0.405	0.330	0.347	0.312	0.166	0.298	0.116	0.402		
$\cos \theta_-^r$		0.478	0.519	0.608	0.521	0.617	0.659	0.642	0.307	0.791	0.688	0.242	0.422		
$\cos \theta_+^k \cos \theta_-^k$		0	0	0	0	0	0	0	0	0	0	0	0		
$\cos \theta_+^n \cos \theta_-^n$		0	0	0	0	0	0	0	0	0	0	0	0		
$\cos \theta_+^r \cos \theta_-^r$		0.0158	0.00747	0.00295	0.000387	$3.26 \cdot 10^{-5}$	$1.08 \cdot 10^{-6}$	$1.78 \cdot 10^{-6}$	0.110	0.0165	0.0552	0.00585	0.00203		
$\cos \theta_+^k \cos \theta_-^k + \cos \theta_+^n \cos \theta_-^n$		0.0519	0.0653	0.0682	0.0370	0.137	0.0961	0.0216	0.178	0.0499	0.0931	0.0549	0.131		
$\cos \theta_+^k \cos \theta_-^k - \cos \theta_+^n \cos \theta_-^n$		0.393	0.317	0.491	0.285	0.352	0.200	0.310	0.614	0.521	0.664	0.427	0.510		
$\cos \theta_+^n \cos \theta_-^n + \cos \theta_+^k \cos \theta_-^k$		0.463	0.297	0.509	0.532	0.512	0.489	0.431	0.336	0.353	0.415	0.329	0.474		
$\cos \theta_+^n \cos \theta_-^n - \cos \theta_+^k \cos \theta_-^k$		0.888	0.627	0.755	0.399	0.907	0.994	0.989	0.980	0.990	0.997	0.987	0.812		
$\cos \theta_+^r \cos \theta_-^r + \cos \theta_+^k \cos \theta_-^k$		0.406	0.445	0.228	0.578	0.821	0.553	0.762	0.000329	0.00870	0.00605	0.0204	0.0391		
$\cos \theta_+^r \cos \theta_-^r - \cos \theta_+^k \cos \theta_-^k$		0.339	0.658	0.447	0.364	0.727	0.516	0.471	0.843	0.725	0.842	0.779	0.860		

References

- [1] Particle Data Group. Review of particle physics. *Chinese physics C*, 40(10):100001, 2016.
- [2] Roger Felipe Naranjo Garcia. *Measurements of top-quark properties at 8 TeV using the ATLAS detector at the LHC*. PhD thesis, Universität Wuppertal, Fakultät für Mathematik und Naturwissenschaften Physik Dissertationen, 2017.
- [3] Adrián Irles Quiles. *Determination of the top-quark pole mass using $t\bar{t} + 1 - jet$ events with the ATLAS detector at the LHC*. PhD thesis, University of Valencia, 2014.
- [4] A. Aguilar et al. Evidence for neutrino oscillations from the observation of $\nu^- e$ appearance in a $\nu^- \mu$ beam. *Physical Review D*, 64(11):112007, 2001.
- [5] Stephen P. Martin. A supersymmetry primer. *Adv. Ser. Direct. High Energy Phys*, 21(515):1–153, 2010.
- [6] Howard Georgi and Sheldon L. Glashow. Unity of all elementary-particle forces. *Physical Review Letters*, 32(8):438, 1974.
- [7] Rabindra N. Mohapatra and Goran Senjanović. Neutrino masses and mixings in gauge models with spontaneous parity violation. *Physical Review D*, 23(1):165, 1981.
- [8] CDF Collaboration. Evidence for a mass dependent forward-backward asymmetry in top quark pair production. *Physical Review D*, 83(11):112003, 2011.
- [9] Werner Bernreuther, Dennis Heisler, and Zong-Guo Si. A set of top quark spin correlation and polarization observables for the LHC: Standard Model predictions and new physics contributions. *Journal of High Energy Physics*, 2015(12):26, 2015.
- [10] ATLAS Collaboration. Measurements of top quark spin observables in $t\bar{t}$ events using dilepton final states in $\sqrt{s} = 8$ tev pp collisions with the ATLAS detector. *arXiv preprint arXiv:1612.07004*, 2016.
- [11] F. Abe et al. Observation of top quark production in p p collisions with the Collider Detector at Fermilab. *Physical review letters*, 74(14):2626, 1995.
- [12] CDF Collaboration. Observation of the top quark. *Physical Review Letters*, 74(14):2632, 1995.
- [13] Taesoo Song and Hamza Berrehrah. Hadronization time of heavy quarks in nuclear matter. *Physical Review C*, 94(3):034901, 2016.
- [14] G. Branco et al. Theory and phenomenology of two-higgs-doublet models, phys. rept. 516 (2012) 1–102. *arXiv preprint arXiv:1106.0034*, 136.

- [15] ATLAS collaboration. Search for heavy Higgs bosons a/h decaying to a top quark pair in pp collisions at $\sqrt{s}=8$ tev with the ATLAS detector. *arXiv preprint arXiv:1707.06025*, 2017.
- [16] DESY. Dealing with systematics for chi-square and for log likelihood goodness of fit statistics. <http://www.desy.de/~blobel/banff.pdf>, 2006.